Inorganic Chemistry

Article

pubs.acs.org/IC

Electrocatalytic and Photocatalytic Conversion of CO_2 to Methanol using Ruthenium Complexes with Internal Pyridyl Cocatalysts

David J. Boston,[†] Yeimi M. Franco Pachón,[‡] Reynaldo O. Lezna,*[,‡] N. R. de Tacconi,[†] and Frederick M. MacDonnell*[,†]

[†]Department of Chemistry and Biochemistry, The University of Texas at Arlington, Arlington, Texas 76019-0065, United States

[‡]Instituto de Investigaciones Fisicoquímicas Teóricas y Aplicadas (INIFTA, UNLP, CCT La Plata-CONICET), Sucursal 4, C.C. 16, (B1906ZAA) La Plata, Argentina

Supporting Information

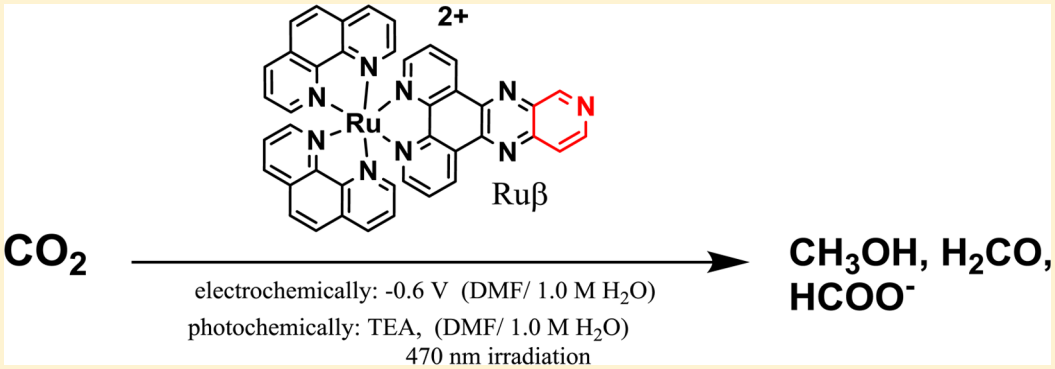

ABSTRACT: The ruthenium complexes $[Ru(phen)_2(ptpb\alpha)]^{2+}$ (Ruα) and $[Ru(phen)_2(ptpb\beta)]^{2+}$ (Ruβ), where phen =1,10-phenanthroline ; ptpbα = pyrido[2′,3′:5,6]pyrazino[2,3-*f*][1,10]phenanthroline; ptpbβ = pyrido[3′,4′:5,6]pyrazino[2,3-*f*][1,10]phenanthroline, are shown as electrocatalysts and photocatalysts for CO_2 reduction to formate, formaldehyde, and methanol. Photochemical activity of both complexes is lost in water but is retained in 1 M H_2O in DMF. Controlled current electrolysis of a solution of Ruβ in CO_2 saturated DMF:H_2O (1 M) yields predominantly methanol over a 6 h period at ∼ −0.60 V versus Ag/AgCl, with traces of formaldehyde. After this time, the potential jumped to −1.15 V producing both methanol and CO as products. Irradiation of Ruβ in a solution of DMF:H_2O (1 M) containing 0.2 M TEA (as the sacrificial reductant) yields methanol, formaldehyde, and formate. Identifications of all of the relevant redox and protonated states of the respective complexes were obtained by a combination of voltammetry and differential reflectance measurements. Spectroelectrochemistry was particularly useful to probe the photochemical and electrochemical reduction mechanisms of both complexes as well as the complexes speciation in the absence and presence of CO_2.

INTRODUCTION

In light of the increasing concerns about global atmospheric CO_2 levels and the dependence of modern society on cheap energy, i.e., fossil fuels, technological advances in the photochemical or electrochemical reduction of CO_2 to liquid fuels could be an important component of a carbon neutral fuel cycle.[1−5] Reduction of CO_2 by transition metal complexes under modest (near ambient) conditions has been explored for decades, with most recent attention focused on coupling this process to electrochemical and/or photochemical methods.[5−16] Some of the seminal early studies include a report by Meyer and co-workers showing that Rh and Ir polypyridyl complexes are competent electrocatalysts for CO_2 reduction to formate in DMF under air-free, ambient conditions.[17] Since then, there have been significant contributions in both electrocatalytic and photocatalytic CO_2 reduction studies by a number of groups including Meyer,[4,18−23] Fujita,[24−28] Kubiak,[29,30] Saveant,[12] Abruna,[31−34] Bocarsly,[35−39] and Crabtree[40] among others.[5,6,11,16]

Of the various strategies toward catalytic CO_2 reduction, the work of Bocarsly[35−39] stands out for its use of a simple organic electrocatalyst, such as pyridine, to produce the 6-electron reduced product methanol over the more common 2-electron reduced products CO and formate.[37,39] The direct production of a viable liquid transportation fuel like methanol from CO_2 has obvious advantages over other technologies that are only showing a 2-electron reduction leading to CO or formate. It is theorized that this six-electron process occurs in a sequentially manner starting with the reduction of the pyridinium cation (pyH^+) to the neutral radical ($pyH^•$), which is followed by insertion of CO_2 into the NH bond to give a radical carbamate

Received: January 8, 2014
Published: June 9, 2014

   dx.doi.org/10.1021/ic500051m | *Inorg. Chem.* 2014, 53, 6544−6553

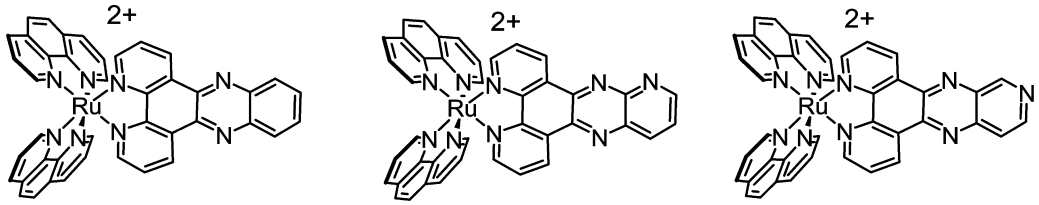

Figure 1. Structures of $[(phen)_2Ru(ptpb\alpha)]^{2+}$ and $[(phen)_2Ru(ptpb\beta)]^{2+}$ complexes and $[(phen)_2Ru(dppz)]^{2+}$ complex.

intermediate.[37,41] Subsequent sequential reductions lead to the final product.

We recently showed that pyridine and $[Ru(phen)_3]^{2+}$ can work in a homogeneous photochemical CO_2 reduction process to produce both formate and methanol, using ascorbic acid as the sacrificial donor.[42] While this photochemical process has poor selectivity for methanol production, favoring formate, it did demonstrate that the pyridinium-based catalysts can reduce CO_2 to methanol in the absence of a metal surface, which had previously been debated as essential or not in some recent theoretical works.[43−45]

The success of this initial bimolecular photocatalytic system led us to examine unimolecular photocatalysts incorporating both the ruthenium chromophore and the pyridyl subunit. In this Article, we evaluate the performance of Ruα and Ruβ (shown in Figure 1) as electrocatalysts and photocatalysts for the reduction of CO_2 in mixed DMF:H_2O (1 M). DMF was chosen as main solvent because the photo-excited-state of these complexes is rapidly quenched in aqueous solvents, but can be appreciable in mixed solvent systems of water and nonprotic solvents.[46] This has an additional advantage in that the solubility of CO_2 in DMF is appreciably higher than in water (0.2 M vs 0.03 M). Using a combination of voltammetry and differential reflectance measurements, we elaborate on the electrochemical and photochemical reduction mechanism and complexes speciation in the absence (N_2 saturated) and presence of CO_2. Constant-current electrolyses and constant irradiation photolysis along with gas chromatography determined methanol to be one of the CO_2 reduction products.

EXPERIMENTAL SECTION

Synthesis. Ruthenium(III) chloride was purchased from Pressure Chemical (Pittsburgh, PA) and used as received. DMF, ethanol, and acetone were purchased from VWR and used as received. Ammonium hexafluorophosphate and 1,10-phenanthroline were purchased from Alpha Aesar and used as received; 3,4-diaminopyridine, 2,3-diaminopyridine, and phenylenediamine were purchased from Sigma-Aldrich and used as received. $[Ru(phen)_2(ptpb\beta)](PF_6)_2$, $[Ru(phen)_2(ptpb\alpha)](PF_6)_2$, and $[Ru(phen)_2(dppz)](PF_6)_2$ were synthesized according to standard proceedures.[47,48]

Electrochemistry and Spectroelectrochemistry. Electrochemical data were obtained by using cyclic (CV) and differential pulse voltammograms (DPV) on a CHI620C electrochemical analyzer (CH Instruments, Austin, TX) using a single compartment (3 mL volume) electrochemical cell. A glassy carbon (1.5 mm diameter disk) working electrode from Cypress Systems was used. The electrode was polished to a mirror finish with wet alumina (Buehler, 0.05 μm), followed by rinsing with Millipore Milli-Q water and sonication. A platinum wire and a Ag/AgCl reference electrode (Cypress, model EE009) were used as counter and reference electrodes, respectively. The electrolyte solutions contains the ruthenium complex in DMF:H_2O (1 M) containing 0.1 M tetrabutylammonium hexafluorophosphate ($TBAPF_6$) as the supporting electrolyte. The solutions were saturated with N_2 or CO_2 prior to each measurement, and the atmosphere was maintained over the electrochemical solution throughout the course of the experiment. All experiments were performed at laboratory ambient temperature (20 ± 2 °C).

Spectroelectrochemistry experiments were performed on a mirror-polished platinum disk as the working electrode. A platinum coil was used as a counterelectrode and was placed in a separate compartment with a fritted end. The reference electrode was a Ag/AgCl, saturated KCl and was used with a Luggin capillary to minimize uncompensated ohmic resistance in the cell. Oxygen was exhaustively removed from the working electrode compartment by bubbling N_2 or CO_2 depending on the particular experiment.

Differential reflectivity in the form of $\delta R/R$ versus potential profiles was recorded on a 2 mV/s potential scan with a superimposed, small amplitude sinusoidal, potential perturbation (ca. 50 mVp-p, 11 Hz). Monochromatic light of a desired wavelength was reflected off the working electrode, and focused on a photomultiplier operating at a constant current set by a feedback system and a programmable power supply. Alternating current voltammetry was used in some cases along with $\delta R/R$ measurements. The rectified ac current and optical ac response (normally the in-phase component) were monitored, after demodulation with a lock-in amplifier, as a function of the electrode potential.[49−51]

Photochemical Reduction. Two types of photochemical experiments were conducted: (i) an absorption experiment looking at the change of the spectra with time irradiation, and (ii) a photocatalysis experiment where a more concentrated solution was irradiated and analyzed for products. For both experiments all solutions were saturated with N_2 or CO_2 gas prior to irradiation. These solutions were then irradiated with a custom built photoreactor[42] using point source lights emitting at 470 nm ±20 nm with a photon flux of 1×10^{-5} Einsteins/second, as measured by chemical actinometry using potassium ferrioxalate.[52] Solution components and concentrations are described in the text. For the photocatalysis experiments, periodic 5.0 mL aliquots were withdrawn by syringe and placed in airtight vials, where they were kept at −20 °C until analyzed by head space GC/MS analysis as described below.

Constant-Current Electrolysis. A two-compartment cell with a large area reticulated vitreous carbon (RCV) cylindrical working electrode (BASI MF-2077) contacted with a platinum wire was placed in the cell's main compartment along with the reference electrode. Platinum foil (2 cm × 8 cm) was used as the counter electrode and was placed within an inner compartment separated by a glass frit from the main compartment. The working electrode compartment contained 0.30 mM of the respective ruthenium complex in DMF:H_2O (1 M) solution with 0.1 M $TBAPF_6$ as supporting electrolyte. The counter electrode compartment contained the supporting electrolyte solution but no ruthenium complex. The cell was saturated with CO_2 and kept pressurized and sealed while the electrolyses were performed at an applied current of −0.6 mA.

Product Detection. Gas chromatography (GC) and colorimetric tests were adopted to analyze the conversion of CO_2 to organic products. A Shimadzu GC with mass spectrometer detector (GC-MS-2010 Plus chromatograph with a MS TQ8030 detector) and an AOC-5000 Plus autosampler was used. The chromatographic column (SHRX105MS, 30-m length and 0.25 mm inner diameter) at an oven

dx.doi.org/10.1021/ic500051m | Inorg. Chem. 2014, 53, 6544−6553

temperature of 45 °C was used in combination with a MS detector at 250 °C; helium was the carrier gas. Detection at m/z = 31, 29, 28, and 45 was chosen to identify methanol, formaldehyde, carbon monoxide, and formate, respectively, as the reaction products. Sample aliquots were preheated at 80 °C in a 20 mL headspace vial with a septa cap, and 2.5 mL of the head space gas was injected from a syringe heated to 80 °C and analyzed in the GC/MS instrument. Control samples containing known concentrations of methanol (in the range 5−1000 μM) were analyzed to obtain a standard curve (Supporting Information Figures S1 and S2).

A quantitative colorimetric procedure (chromotropic acid test) was used for formaldehyde and formic acid detection (see Supporting Information Figure S3).[31,35,53] First, liquid samples were treated with Amberlite IRN-150 ion-exchange resin to remove the ruthenium complex. As this test is for aldehyde detection, the sample was divided, and formaldehyde concentration was determined from one-half. Subsequently, 0.5 mL aliquots of the other half were treated with magnesium turnings under acidic conditions to reduce the formic acid to formaldehyde.[53] After determination of the new formaldehyde concentration, formic acid concentration was determined by difference.

RESULTS AND DISCUSSION

Approach for Photo- and Electrocatalytic CO_2 Reduction by Ruα and Ruβ. Ruα, and Ruβ share structural similarities with Rudppz (Figure 1) which are manifest in that all three complexes are weak or nonemitting in aqueous solution, but exhibit strong (or bright) emission in nonprotic solvents, such as MeCN and DMF. Mixed-aqueous solutions (i.e., DMF:water) show intermediate behavior with luminescence intensity and lifetimes falling with increasing water concentration.[46,54] For example, a Rudppz solution containing 1 M water in DMF displays a lifetime on the order of 400 ns compared to 250 ps in pure water; thus, it is possible to access the photoexcited molecule for photochemical reactions in solutions with appreciable (up to 1M) amounts of water.

The variability of the luminescence lifetimes in these complexes is attributed to the presence of two energetically similar triplet excited-states, the $^3MLCT_{prox}$ and $^3MLCT_{dist}$, which formally localize the excited electron in a proximal[55−57] "bpy-like" MO on the extended ligand or in a distal "phenazine-like" MO, respectively. In aqueous solution, Rudppz emission is weak and red-shifted (~670 nm, $\phi_{lum} = 2.5 \times 10^{-6}$) relative to that in MeCN (610 nm, $\phi_{lum} = 0.033$)[52] due to population of the $^3MLCT_{dist}$ state being favored in water and the $^3MLCT_{prox}$ state being favored in MeCN. As the proportion of water is increased in the mixed solvent system, the increased polarity of the solvent is better able to stabilize the large excited-state dipole in the $^3MLCT_{dist}$ shifting the excited-state equilibration between the two states more toward the short-lived $^3MLCT_{dist}$ state.[46,54−56] As Ruα and Ruβ exhibit largely analogous luminescent behavior, it is thought that they have similarly behaving $^3MLCT_{prox}$ and $^3MLCT_{dist}$ excited-states.[55,56]

Electrochemistry. Figure 2 compares differential pulse voltammograms (DPV) in N_2 saturated DMF:H_2O (1 M) encompassing the electroreduction of Ruα (green solid line), $[Ru(phen)_3]^{2+}$ (red dash line), and pyridine (blue dash dot line). The Ruα complex shows three main electroreduction processes while two are detected for complex $[Ru(phen)_3]^{2+}$ and no electrochemical activity is seen for pyridine and in agreement with previously reported data.[58] For the parent $[Ru(phen)_3]^{2+}$ complex only two sharp peaks are shown at −1.13 and −1.26 V, respectively; they are associated with two sequential 1-electron uptakes, one in each phen-like MO[59] while the third electron uptake is located at more negative

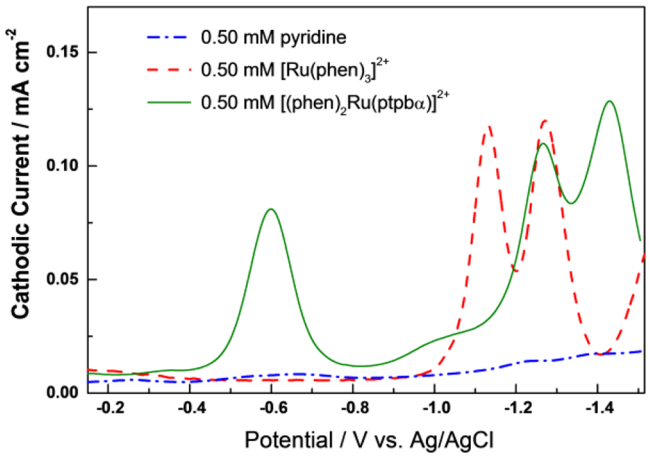

Figure 2. Comparison of DPV runs for $[(phen)_2Ru(ptpb\alpha)]^{2+}$, $[Ru(phen)_3]^{2+}$, and pyridine encompassing the electroreduction potential range (−0.15 V to −1.5 V) recorded at a glassy carbon disc electrode in DMF:H_2O (1 M) solution saturated with N_2. Reactant concentration = 0.5 mM, supporting electrolyte = 0.1 M $NBu_4^nPF_6$.

potentials than those depicted in Figure 2. With respect to complex Ruα, the first redox process is located at ca. −0.61 V and is followed by a low shoulder at ca. −1.0 V and two next sharp peaks appearing at −1.22 and −1.43 V, respectively. In concurrence with the voltammetric profile of $[Ru(phen)_3]^{2+}$, the last two processes in Ruα are associated with two sequential electron uptakes in the two phen ligands, but the two more positive waves are assigned to electroreduction of the ptpbα ligand.

The cyclic voltammograms (CVs) for Ruα and Ruβ in the initial reduction region are overlaid in Figure 3. As can be seen, the first reductive redox process for Ruα and Ruβ in N_2 saturated DMF:H_2O (1 M) shows highly reversible voltammetric waves (v = 50 mV/s) at redox potentials, E^0, of −0.64 and −0.57 V versus Ag/AgCl, respectively (Figure 3a). These reductions are assigned to reduction of the ptpbα and ptpbβ ligands, and are found at slightly more positive potentials than observed for Rudppz (located at −0.81 V vs Ag/AgCl) in dry DMF and at −0.80 V after addition of water.[60] The potential positive shift in Ruα and Ruβ is reasonable given the extra nitrogen in these ligands relative to dppz increases the overall electronegativity of the ligand. Figure 3b shows the effect of concentration of complex Ruα on CVs spanning the first electroreduction process. The concentration was varied from 0.05 to 0.30 mM. The shape of the voltammograms and the peak separation afford a Nernstian (reversible) behavior under diffusion control for this complex in the absence of CO_2. From the linear slope of the cathodic current peak with complex concentration (inset to Figure 3b), it was determined that it is a one-electron process, assuming a diffusion coefficient of 3×10^{-6} cm^2/s.[61]

A Pourbaix diagram of the first electroreduction process for Ruβ was obtained in water to determine if and when the reduction is coupled to protonation (see Supporting Information Figure S4). The pK_a of the conjugate acid $[Ru(phen)_2(ptpb\beta H)]^{3+}$ (RuβH) was determined to be 3.3, and the slope (m = −62 mV/pH) of the redox process at pH > 3.3−7.0 indicates a one-electron, one-proton process. We note that this behavior is different from that observed with pyridine as the pH is varied, which instead shows a larger peak current but no significant potential shift (see Supporting Information

dx.doi.org/10.1021/ic500051m | Inorg. Chem. 2014, 53, 6544−6553

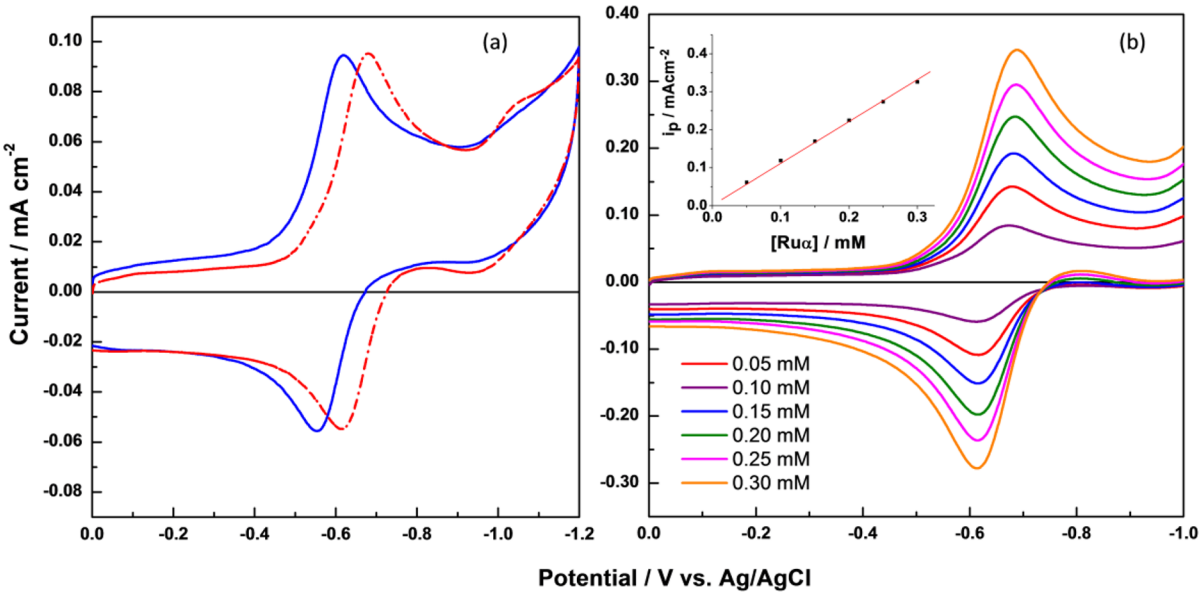

Figure 3. (a) Comparison of the cyclic voltammetric behavior of Ruα (red dash line) and Ruβ (blue solid line) in N_2 saturated DMF:H_2O (1 M) solutions. Working electrode: glassy carbon disk (1 mm diameter), scan rate = 50 mV/s, complex concentration = 20 μM, supporting electrolyte = 0.1 M $TBAPF_6$. (b) Effect of concentration on the voltammetric behavior of the first electroreduction process of Ruα in solutions saturated with N_2. The increase of the cathodic current peak with the complex concentration follows a linear relationship (shown in the inset plot).

Figure S5a,b). This latter behavior has been suggested to show the reduction of hydrated protons[62] and, importantly, is absent in our electrocatalysts. A similar Pourbaix analysis for Rudppz and Ruα revealed the pK_a's of the conjugate acids are below zero and the electroreduction is also a one-electron, one-proton process out to pH 7. In the mixed solvent, the CV behavior of Ruβ is similar although cathodically shifted from −0.07 V (water pH 4.5) to −0.6 V (DMF:H_2O 1 M) (see Supporting Information Figure S5).

Electrochemistry of Ruα and Ruβ in N_2- and CO_2-Saturated Solutions. Electrocatalytic reduction of CO_2 by Ruα and Ruβ is observed by simply bubbling CO_2 through the DMF:H_2O (1 M) solution and examining the resulting CVs, particularly when performed at low potential scans rates (5−10 mV/s). As seen in Figure 4, large increases in the cathodic current are observed at −0.64 and −0.60 V for Ruα and Ruβ, respectively, indicating electrocatalytic CO_2 reduction. Rudppz, in contrast, is not electrocatalytically active under identical conditions when CO_2 is added (data not shown), indicating the need for the extra nitrogen in the ligand structure for catalytic activity. A control run of CO_2-saturated solution without addition of any of the ruthenium complexes (Figure 4, black dot trace) indicates that the glassy carbon electrode is not active for CO_2 reduction. In the absence of a catalyst and in media of low proton availability (such as DMF and DMSO), electroreduction of CO_2 is reported to occur at −2.16 V versus Ag/AgCl.[63]

In both Ruα and Ruβ, the presence of a distal nitrogen site on the ptpb (either α or β) is postulated to be responsible for the catalytic activity as the Rudppz complex was found electrocatalytically inactive. This pyridyl-like moiety appears to be needed to form the initial CO_2 adduct, presumably in the form of a carbamate-type radical intermediate.[37] Figure 4 also shows a net increase of cathodic current at potentials more negative than −1.1 V for both complexes, indicating that the reduction of CO_2 is also catalytically occurring at these potentials. A comparison of DPV runs for Ruα and [Ru-

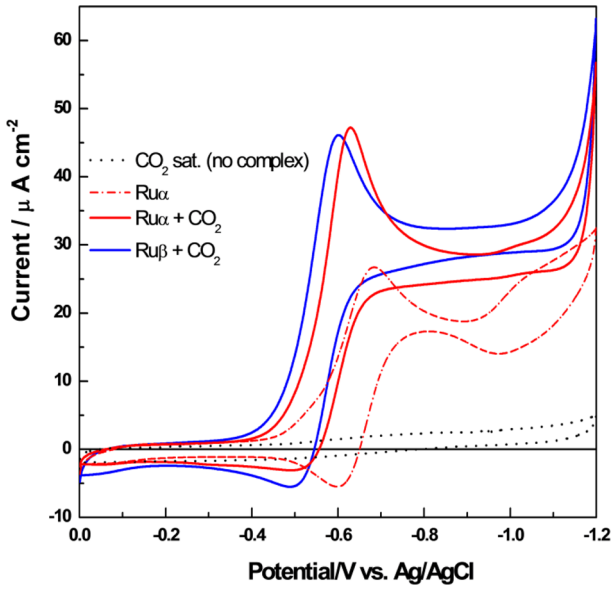

Figure 4. Comparison of the voltammetric behavior of Ruα (red solid line) and Ruβ (blue solid line) in DMF:H_2O (1 M) solutions saturated with CO_2. Voltammograms of Ruα before saturation with CO_2 (red dash line) and that without Ru complex but with CO_2 (black dot line) are included as reference. All voltammograms were run at 5 mV/s with a glassy carbon working electrode.

$(phen)_3]^{2+}$ both in N_2 and CO_2 saturated solutions, shown in Supporting Information Figure S6, reveals only the former is catalytic, at potentials greater than −1.4 V indicating the ptpb ligand is integral to the catalysis at −0.6 and −1.2 V. Moreover, the catalytic mechanism for CO_2 electroreduction was corroborated by plotting the Nicholson−Shain current peak function ($i_p/v^{1/2}$) versus the scan rate (v) for Ruβ^{2+} complex in DMF:H_2O (1 M) saturated with CO_2 (Supporting Information Figure S7).[64]

dx.doi.org/10.1021/ic500051m | Inorg. Chem. 2014, 53, 6544−6553

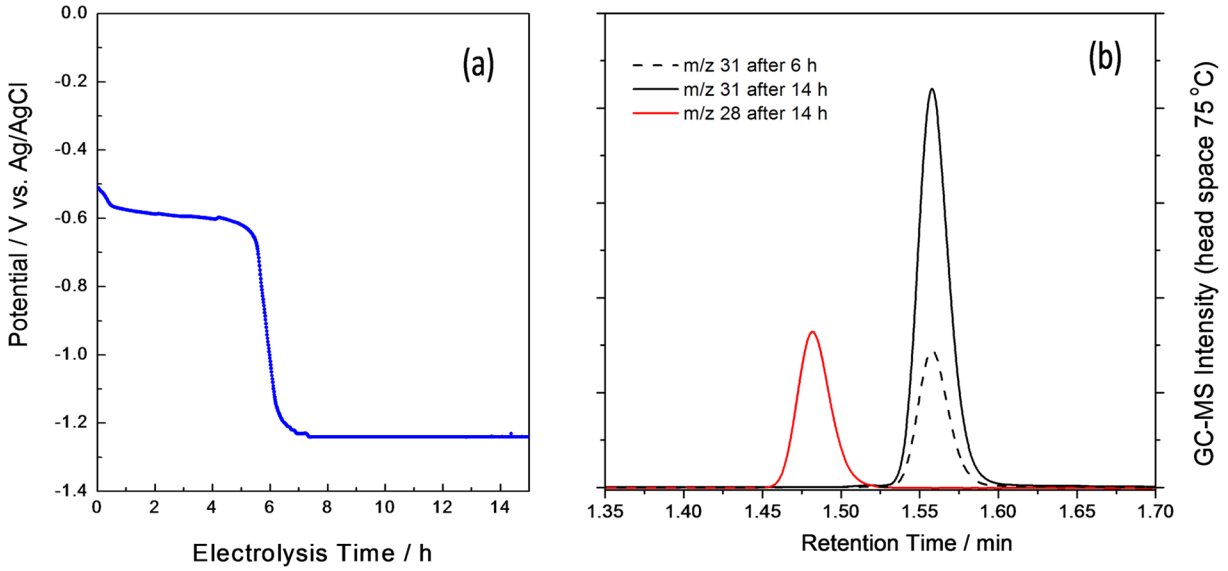

Figure 5. (a) Potential/time profile recorded during cathodic galvanostatic electrolysis of Ruβ (0.30 mM) in DMF:H_2O (1 M) saturated with CO_2. (b) Head space GC/MS analyses of liquid aliquots removed after 6 and 14 h of electrolysis, respectively. MS peak intensities at 1.56 min (m/z = 31) from CH_3OH increase ca. 2.5 times from 6 to 14 h of electrolysis. Formation of CO (m/z = 28, at 1.47 min, red trace) is only present after the potential has evolved to ca. −1.2 V. Electrolysis conditions: 0.1 M $TBAPF_6$ (0.1 M) as supporting electrolyte; working electrode = RVC cylindrical electrode; applied current = −0.6 mA.

Table 1. Comparison of Two Photosystems That Make Methanol. (a)

		MeOH			formaldehyde			formate		
system	Ru μmol	μmol	TON (in e^-)	$\Phi \times 10^{-5}$	μmol	TON (in e^-)	$\Phi \times 10^{-3}$	μmol	TON (in e^-)	$\Phi \times 10^{-3}$
Ruβ DMF:water (2.5 μmol)	2.5	1.1 ± 0.2 (n = 4)	0.4 (2.6)	15	7.1	2.8 (11.4)	1.6	16.2	6.5 (13)	3.6
$[Ru(phen)_3]^{2+}$:py 1:200 (6 μmol Ru)[a]	6	0.9 ± 0.08	0.15 (0.9)	6.3				55	9 (18)	3
$[Ru(phen)_3]^{2+}$:py 1:200 (0.1 M KCl) (6 μmol Ru)[a]	6	1.7 ± 0.3	0.3 (2.0)	11				450	76 (152)	25

[a]Data from ref 41.

In the absence of substrate (CO_2), we observe a second reductive redox process for Ruα at −1.05 V which is strongly attenuated when CO_2 is present (Figure 4 and Supporting Information Figure S6). The magnitude of this follow-up wave increases at lower scan rates, which is suggestive of dimerization of the radical $[Ru^{II}(phen)_2(ptpb\alpha^{\bullet})]^+$, where (ptpb$\alpha^{\bullet}$) is the one-electron reduced ptpbα ligand, as shown in reaction 1, and that the new dimer is the resulting electroactive species. Radical dimerization is not uncommon in these systems and has been reported previously in closely related complexes.[60,65−67]

$$Ru\alpha^{\bullet} + Ru\alpha^{\bullet} \rightarrow (Ru\alpha)_2 \quad (1)$$

The lack of a similar secondary redox process in the CV of Ruβ suggests that this complex is not subject to this dimerization side-reaction and hints that the site of dimerization is the distal carbons on ptpbα.

Product Analysis of Electrocatalytic and Photocatalytic CO_2 Reduction. In order to determine the products of CO_2 reduction, Ruβ was subjected to controlled-current electrolysis in CO_2-saturated DMF:H_2O solution. As CV studies revealed typical diffusion control behavior for the first electron uptake in Ruβ at concentrations ≤0.30 mM, the bulk electrolysis was performed under similarly dilute concentrations in order to minimize potential side reactions, such as dimerization. A representative potential−time plot obtained during electrolysis is shown in Figure 5a. The electrode potential is seen to stabilize at ca. −0.6 V (first electroreduction process of the complex) for a period of time spanning 6 h, and then the potential is seen to rapidly evolve to more negative values associated with the second electroreduction of the complex and remains there for at least 15 h. Comparison of Figure 5a with the respective DPV run in Figure 2 demonstrates that the two potential arrests in Figure 5a are associated with the respective electroreduction processes tracked in the DPV run (green solid line in Figure 2). The abrupt negative potential shift at 6 h electrolysis signals a change in the electrocatalytic reduction mechanism which curiously corresponds with the production of approximately 1 methanol per Ruβ. Coulometric calculation of the number of electrons consumed in the time period of the first potential plateau (at −0.6 V) is 5.5 electrons per Ruβ. Headspace GC/MS analysis of aliquots collected after 5 h electrolysis (Figure 5b) revealed that 0.92 CH_3OH per Ruβ was produced. No CO was detected at this time but some formaldehyde was detected at m/z 29. While it is unclear what caused this abrupt potential change, it suggests that the ptpbβ ligand in Ruβ is covalently modified such that it can no longer participate in the redox reaction, thus the jump to the next available redox couple. After 14 h of electrolysis, the methanol yield is nearly triple that found at 6 h (Figure 5b); however, a change in mechanism is clear as CO is now observed in the GC/MS with a final product distribution being 75% methanol and 25% CO.

In a photochemical experiment, 25 mL of a 100 μM Ruβ solution in DMF:H_2O (1 M) with 0.1 M TEA was saturated

dx.doi.org/10.1021/ic500051m | Inorg. Chem. 2014, 53, 6544−6553

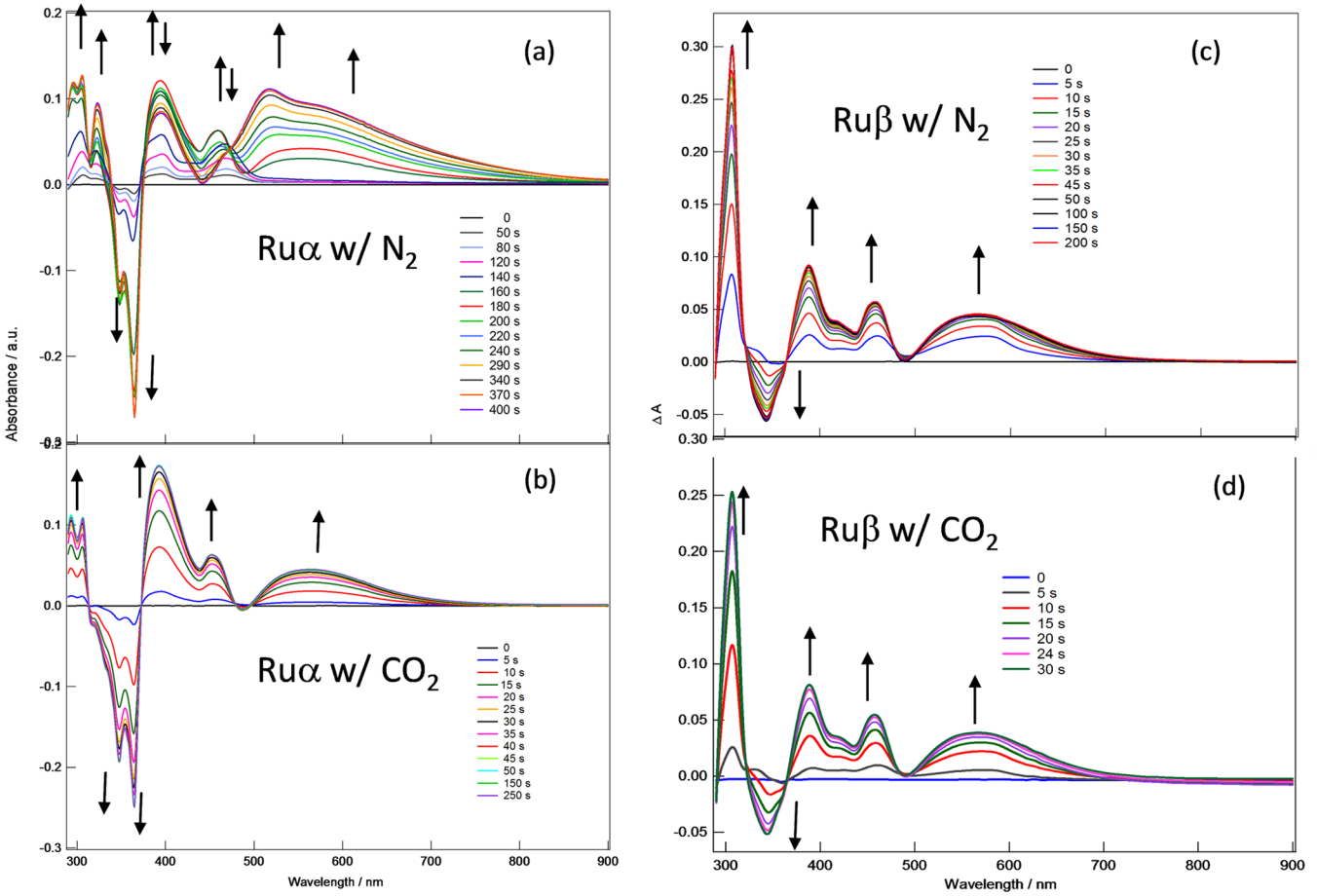

Figure 6. Transient ΔA spectra of Ruα (22 μM) during photolysis in N_2 (a) and in CO_2 (b) saturated DMF:TEA (0.25 M)/H_2O (1 M) solutions and Ruβ (22 μM) during photolysis in N_2 (c) and in CO_2 (d) saturated DMF/TEA (0.25 M)/H_2O (1 M) solutions. Peaks pointing down indicate bands disappearing while those pointing up correspond to new bands appearing due to photolysis.

with CO_2 and irradiated with 470 nm light for up to 6 h at 25 °C. A color change is apparent after 90 min, and the solution is appreciably darker after 6 h. Product analysis at the 1 h time point yielded 16.2 μmol formate, 7.1 μmol formaldehyde, and 1.1 μmol methanol solution, as shown in Table 1. At longer irradiation periods (ca. 8 h), the methanol has only increased to 1.5 μmol indicating that the system deactivation is apparently coupled to the color change, which is likely due to ligand labilization.[68] A comparison of products for the bimolecular $[Ru(phen)_3]^{2+}$–pyridine photosystem[42] and Ruβ after 1 h irradiation is given in Table 1 and reveals that Ruβ is slightly superior as a methanol producing photocatalyst in terms of quantum yield. The turnover number (TON) in the first hour for Ruβ is 27 on an electron basis, which is broken down to 0.4 for MeOH (6 e^- product), 2.8 formaldehyde (4 e^- product), and 6.5 formate (2 e^- product), compared to 154 on an electron basis for the $[Ru(phen)_3]^{2+}$–pyridine system. While Ruβ is apparently less active than the $[Ru(phen)_3]^{2+}$–pyridine system, it is more selective for methanol, producing more in the first hour on both an absolute quantum yield basis and relative basis (9% of the reducing equivalents end up in MeOH for Ruβ vs 1% for the Ru:pyridine system). These comparisons need to be considered with the caveat that solvent systems are different in the two cases.

Effect of CO_2 on the Photochemistry of Ruα and Ruβ complexes. As the ability of Ruβ to function as a CO_2 reduction photocatalyst was established, we attempted to see if we could detect any of the likely intermediates by examining the evolution of the UV–vis absorption spectrum in the range 300–900 nm as a function of irradiation time in the presence and absence of CO_2. The differential absorption (ΔA) data for Ruα and Ruβ under N_2 or CO_2 atmosphere as a function of the irradiation time are shown in Figure 6. The initial absorption spectra for Ruα and Ruβ in a CO_2-saturated solution containing 0.25 M TEA (sacrificial donor) before and after visible light irradiation are shown in Supporting Information Figure S8a,b, respectively. Observe in Figure 6 that Ruα and Ruβ show differences in the evolution of their ΔA spectra in N_2 but are nearly identical in their evolution in the presence of CO_2.

Moreover, there is little noticeable difference in the evolution of the ΔA spectra for Ruβ under N_2 or CO_2 (Figure 6c,d, respectively) upon irradiation. The changes seen under a N_2 atmosphere are consistent with the formation of a one-electron reduced, protonated complex $[(phen)_2Ru^{II}(ptpb\beta H^{\bullet})]^{2+}$ (RuβH$^{\bullet}$). The observed spectral changes are characteristic of ligand reduction in ruthenium(II) coordinated dppz complexes and in related complexes with extended phenazine-like ligands.[55−57,60,69,70] Reduction is associated with a ligand bleach around 350 nm and a broad new absorption band around 560 nm. From Figure 6d, it would appear that RuβH$^{\bullet}$ (detected at 564 nm) is also the product of photoreduction under a CO_2 atmosphere except for two subtle differences. The final spectrum obtained under CO_2 is slightly attenuated

dx.doi.org/10.1021/ic500051m | Inorg. Chem. 2014, 53, 6544−6553

relative to that seen under N_2, and the growth of the peak at 564 nm is slightly slower under CO_2.

The more complicated evolution of the ΔA spectra for Ruα under N_2 (shown in Figure 6a) is seen more clearly in Figure 7

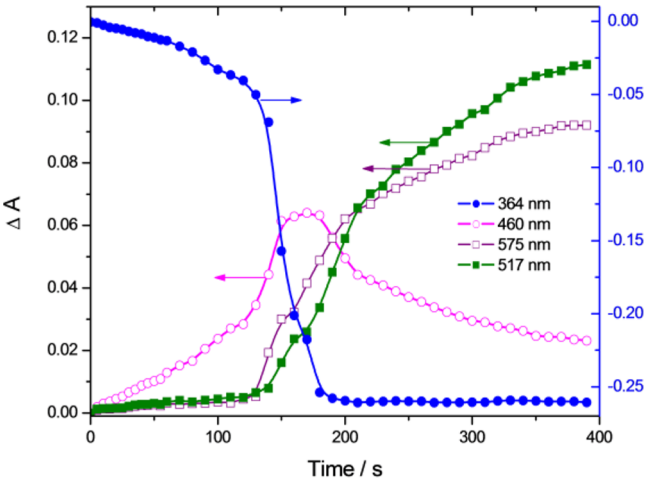

Figure 7. Absorbance versus time for selected wavelengths for Ruα under nitrogen atmosphere upon irradiation. Data taken from Figure 6a.

in which the absorbance at 364 nm (ptpbα bleach), 460 nm (intermediate band), 517 nm (final new product band), and 575 nm (radical anion band) are plotted versus irradiation time. The intermediate is assigned to formation of the dimer, $(Ru\alpha)_2$, which itself can be further reduced to yield a product with similar spectral features to Ru$\alpha^{\bullet}$ or RuαH$^{\bullet}$. Formation of this final product has the broad absorption feature between 500 and 800 nm, plus it introduces a distinct new absorption peak at 517 nm which is not seen in the radicals of the monomeric RuαH$^{\bullet}$ or RuβH$^{\bullet}$. We have similar behavior in the radical dimerization reactions of the radicals of $[(bpy)_2Ru(tatpp)]^{2+}$, where tatpp is tetraazatetrapyridopentacene.[65] Under a CO_2 atmosphere, the dimerization reaction (shown by a band at 517 nm) is inhibited under both electrochemical (Figure 4) and photochemical (Figure 6b) conditions. The final ΔA spectrum in Figure 6b is very similar to that seen for Ruβ in Figure 6c,d, suggesting that the final product here is RuαH$^{\bullet}$.

From the spectral data seen in Figure 6 b–d, it appears that CO_2 is not interacting with the radical products RuαH$^{\bullet}$ and RuβH$^{\bullet}$, as there are no obvious spectral differences in the 300–900 nm window. However, since Ruα does not show significant signs of dimerization when CO_2 is present, it is clear that CO_2 has some interaction with the reduced complexes. These contradictory data can be interpreted if we posit that there is fast and reversible formation of a CO_2-radical adduct, as shown in reaction 2, and the rate of photoreduction is significantly greater than the subsequent CO_2 reduction reactions of the adduct. This initial equilibrium inhibits dimer formation in the case with Ruα.

To examine the photocatalyst capability to continuously affect CO_2 reduction, samples of Ruβ prepared as described in Figure 6d were irradiated for 30 s to fully photoreduce the complex; the samples were then kept in the dark for 5 min during which time the original spectrum was regenerated. Re-exposure to light for 30 s showed the process could be repeated without issue (see Supporting Information Figure S9).

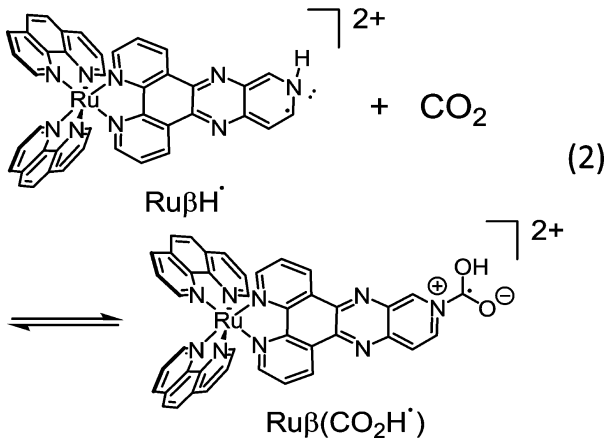

The existence of a fast equilibrium between the complex radical anion and the CO_2 adduct is more clearly seen in the differential reflectance data as a function of potential and is shown in Figure 8. The data for Ruα (at 575 nm, Figure 8a) and Ruβ (at 564 nm, Figure 8b) under N_2 (black lines) and CO_2 (red lines) atmospheres are shown for the forward and reverse scan. The vertical scale is such that the appearance of electrochemically generated species gives rise to positive $\delta R/R$ signals at ~575 nm for Ruα and 564 nm for Ruβ, respectively, regardless of the direction of the scan. While this is a

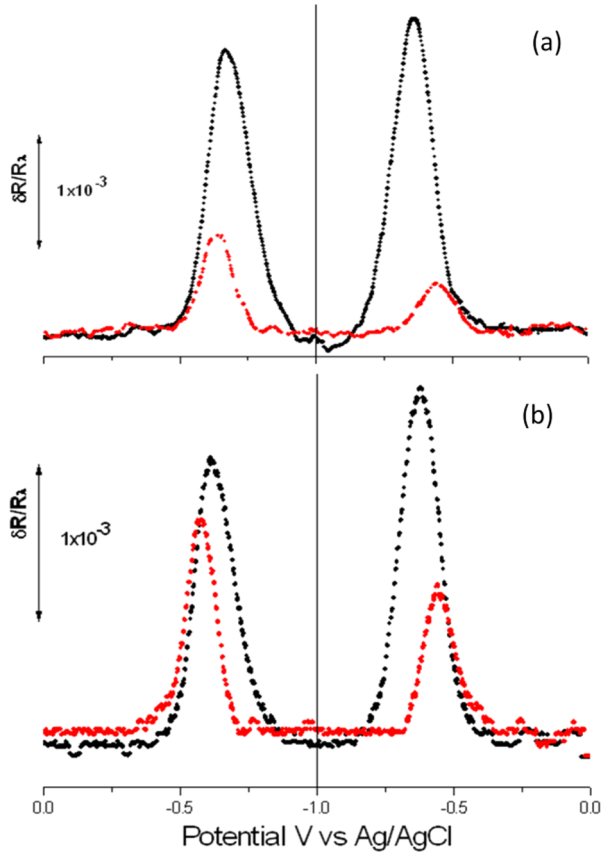

Figure 8. $\delta R/R$ vs potential curves of Ruα at 575 nm (a) and Ruβ at 564 nm (b) in DMF:H_2O containing 0.1 M $TBAPF_6$. These runs were recorded as a function of potentials in degassed (black trace) and CO_2 saturated solutions (red trace). The working electrode was a mirror-polished Pt disc subjected to a sine potential wave (11 Hz, 50 mV_{p-p}) superimposed on a 2 mV/s potential scan.

dx.doi.org/10.1021/ic500051m | Inorg. Chem. 2014, 53, 6544–6553

spectroelectrochemical and not a photochemical experiment, it clearly shows an attenuation and a positive shift of the peak associated with formation of RuαH$^{\bullet}$ and RuβH$^{\bullet}$ in the presence of CO_2. This can be interpreted in terms of the equilibrium expression in reaction 2 for RuβH$^{\bullet}$ or a similar expression for RuαH$^{\bullet}$, if we assume that the 517 nm peak is associated with formation of the dimer species and this peak is absent in the CO_2 adduct (Supporting Information Figure S10). The attenuation is indicative of the equilibria shown in reaction 2, showing the consumption of the electroreduced species (via formation of the CO_2 adduct) in the two cases. The attenuation is more pronounced for Ruα suggesting the equilibrium with the CO_2 adduct (and subsequent follow-up reduction reactions) lies further to the right. The decrease in absorbance, measured as $\delta R/R$, shows that some of the electroreduced species, RuβH$^{\bullet}$ and RuαH$^{\bullet}$, are intercepted by CO_2 in an ECC′-type (catalytic) mechanism, and if we assume a fast equilibration for adduct formation (i.e., reaction 2), then the attenuation reflects the relative equilibrium constants for RuαH$^{\bullet}$ than RuβH$^{\bullet}$ with CO_2, which are estimated at 3 and 1, respectively (assuming a pCO_2 of 1 atm). The larger equilibrium constant seen for RuαH$^{\bullet}$ than RuβH$^{\bullet}$ is in keeping with the relative basicities of the two radical anions (pK_a (RuαH$^{\bullet}$) < pK_a (RuβH$^{\bullet}$)). This interpretation is also supported by the changes in magnitudes seen in the reverse scans. Under a N_2 atmosphere, both Ruα and Ruβ show typical behavior in that the return peak amplitude is larger as the concentration of the electroreduced species has built up during the time spent in the cathodic regime. In contrast, the amplitude of the return peak under a CO_2 atmosphere has diminished relative to the forward scan indicating that this species has been further depleted in an ECC′ mechanism, which would follow if the CO_2 adducts were being consumed on a slower time scale in further reduction reactions, thus shifting the equilibrium position further away from the radical anions, of Ru$\alpha^{\bullet-}$ and Ru$\beta^{\bullet-}$. The positive ca. 50 mV shift seen in the potentials in the presence of CO_2 is due, in part, to the consumption of some of the product in the CO_2 adduct formation and possibly, in part, to small decrease in pH as the presence of CO_2 acidifies the solution. $\delta R/R$/potential curves for complex Ruα were also obtained at 517 nm to explain the photochemical mechanism in the absence and presence of CO_2 (Supporting Information Figure S10). In the absence of CO_2, the species tracked at 517 nm is clearly seen to be formed in the same potential range as that at 575 nm.

From the electrochemical and photochemical data, Ruβ is the better catalyst for CO_2 reduction because it lacks the dimerization side reaction seen for Ruα. Therefore, a catalytic ECC′-mechanism of Ruα and Ruβ complexes to drive CO_2 reduction is perceived as

$$\mathrm{Ru}\varphi + \mathrm{e}^- \rightarrow \mathrm{Ru}\varphi^{\bullet} \quad (\mathrm{Ru}\varphi = \mathrm{Ru}\alpha \text{ or } \mathrm{Ru}\beta) \quad \mathrm{E} \tag{3}$$

$$\mathrm{Ru}\varphi^{\bullet} + \mathrm{H_3O^+} \rightarrow \mathrm{Ru}\varphi\mathrm{H}^{\bullet} + \mathrm{H_2O} \quad \mathrm{C} \tag{4}$$

$$\mathrm{Ru}\varphi\mathrm{H}^{\bullet} + \mathrm{CO_2} \rightarrow \mathrm{Ru}\varphi\mathrm{CO_2H} \quad \mathrm{C'} \tag{5}$$

with reaction 5 competing with dimerization (reaction 1) in the case of Ruα complex.

Reactions 3 and 4 are certainly occurring at the glassy carbon electrode interface, as indicated by cyclic voltammograms of both complexes in N_2 saturated DMF:H_2O as well as in aqueous media at different pH values in the range 6 to 0 (Figure 3 and Supporting Information Figures S4, S5, and S11); the highest pH is chosen because of its proximity to the natural pH of a CO_2 saturated aqueous solution. The voltammetric waves shifting to more positive potentials as the pH decreases and following a Pourbaix plot indicated a 1-electron and 1-proton reaction during the first electroreduction process for both Ruα and Ruβ. The pK_a of both complexes (3.3 for Ruβ and <0 for Ruα) show definitively that, at pH > 3, either in organic or aqueous media, the first process occurring in both is the electron uptake (reaction 3), and that they are not protonated prior to the electroreduction reaction and in contrast with the case of the pyridine as reported by Bocarsly.[38]

The first electroreduction process in Ru complexes containing dppz-like ligands has been shown to be 1-electron and 1-proton processes localized largely on the dppz-like ligand (as indicated in reactions 3 and 4 for our present system) both in organic and water media.[65] For RuβH$^{\bullet}$ and RuαH$^{\bullet}$, the additional pyridyl-type nitrogen couples the site of electron storage with the site of CO_2 adduct formation (reaction 5). The rate constant (k') for reaction 5 can be estimated at 0.14 M^{-1} s^{-1} and 0.33 M^{-1} s^{-1} for Ruα and Ruβ, respectively. These rate constants were calculated from the respective λ values[64] for each complex ($\lambda = (RT/nFv)k'C_{CO2}$) as obtained from voltammetric profiles as those in Figure 4. The product of reaction 5 needs five additional reduction cycles to form one molecule of methanol, the details of which are not yet understood.

In a photochemical cycle, reaction 3 represents reductive quenching of the photoexcited chromophore by the sacrificial donor and from there can similarly react via reactions 4 and 5. Subsequent reductions may occur via excitation of the now modified Ru complex or via electron-transfer from another Ru$\varphi^{\bullet}$. While Ruβ is only a slight improvement over the bimolecular $[Ru(phen)_3]^{2+}$−pyridine system as a photocatalyst in terms of methanol production, it appears to be more selective for methanol production.

CONCLUSIONS

Ruα and Ruβ show that a ruthenium(II) polypyridyl chromophore can be covalently modified with a pendant pyridyl function so as to act as a unimolecular electro- and photocatalyst for CO_2 reduction to deeply reduced products, such as methanol and formaldehyde, in addition to formate. While the extent of photocatalysis is modest, these complexes represent a small but growing family of photocatalysts able to drive CO_2 reduction beyond a simple 2-electron reduction to CO or formate to yield arguably more valuable products such as methanol. Unlike the situation with pyridine as an electrocatalyst, there is nothing unusual about the reduction potentials for Ruα (−0.64 V) and Ruβ (−0.57 V), which are typical for dppz-like ligands when coordinated to the Ru(II) ion. Interestingly, the electrocatalysis is far more selective for methanol production than photocatalysis, perhaps reflecting the ability of the electrode to rapidly provide multiple electrons to the catalyst compared to the photocatalytic cycle. Differential absorbance studies versus time reveal initial products in the photochemical process to be the radicals RuαH$^{\bullet}$ and RuβH$^{\bullet}$, and differential reflectance spectroelectrochemistry shows these products are in rapid equilibration with their CO_2 adducts. The stability of these ruthenium(II) photocatalysts with respect to photolabilization and degradation appears to be the most significant initial challenge in further developing this technology. Projects addressing this aspect of the technology are in progress.

dx.doi.org/10.1021/ic500051m | Inorg. Chem. 2014, 53, 6544−6553

■ ASSOCIATED CONTENT

Supporting Information

Figures regarding quantitative detection and analyses of methanol, formaldehyde, and formate, as well as electrochemical controls and comparisons. This material is available free of charge via the Internet at http://pubs.acs.org.

■ AUTHOR INFORMATION

Corresponding Authors

*E-mail: rolezna@inifta.unlp.edu.ar.

*E-mail: macdonn@uta.edu.

Notes

The authors declare no competing financial interest.

■ ACKNOWLEDGMENTS

The authors thank the NSF for Grants CHE-1301332 and CHE-0840509 (for the purchase of a 500 MHz NMR), the Robert A. Welch Foundation [Grant Y-1301], and BID1728/OC-RA, CONICET PIP #00246 (to R.O.L.), for financial support. We also thank the DOE EERC for financial support to the UTA Center for Renewable Energy Science and Technology (CREST) 2011−2013.

■ REFERENCES

(1) Kumar, B.; Llorente, M.; Froehlich, J.; Dang, T.; Sathrum, A.; Kubiak, C. P. *Annu. Rev. Phys. Chem.* **2012**, *63*, 541−569.

(2) Lewis, N. S.; Nocera, D. G. *Proc. Natl. Acad. Sci. U.S.A.* **2006**, *103*, 15729−15735.

(3) Armaroli, N.; Balzani, V. *Angew. Chem., Int. Ed.* **2007**, *46*, 52−66.

(4) Song, W.; Chen, Z.; Brennaman, M. K.; Concepcion, J. J.; Patrocinio, A. O. T.; Iha, N. Y. M.; Meyer, T. J. *Pure Appl. Chem.* **2011**, *83*, 749−768.

(5) Boston, D. J.; Huang, K.-L.; De Tacconi, N.; Myung, N.; MacDonnell, F. M.; Rajeshwar, K. In *Photoelectrochemical Water Splitting: Materials, Processes and Architectures*; Lewerenz, H. J., Peter, L., Eds.; Royal Society of Chemistry: London, 2013; p 289.

(6) Kelly, C. A.; Mulazzani, Q. G.; Venturi, M.; Blinn, E. L.; Rodgers, M. A. J. *J. Am. Chem. Soc.* **1995**, *117*, 4911−4919.

(7) Jacquet, O.; Frogneux, X.; Das Neves Gomes, C.; Cantat, T. *Chem. Sci.* **2013**, *4*, 2127−2131.

(8) Costentin, C.; Drouet, S.; Robert, M.; Saveant, J. M. *Science* **2012**, *338*, 90−94.

(9) Darensbourg, D. J.; Rokicki, A.; Darensbourg, M. Y. *J. Am. Chem. Soc.* **1981**, *103*, 3223−3224.

(10) Cokoja, M.; Bruckmeier, C.; Rieger, B.; Herrman, W. A.; Kuhn, F. E. *Angew. Chem., Int. Ed.* **2011**, *50*, 8510−8537.

(11) Sato, S.; Koike, K.; Inoue, H.; Ishitani, O. *Photochem. Photobiol. Sci.* **2007**, *6*, 454−461.

(12) Saveant, J.-M. *Chem. Rev.* **2008**, *108*, 2348−2378.

(13) Costentin, C.; Robert, M.; Saveant, J. M. *Chem. Soc. Rev.* **2013**, *42*, 2423−2436.

(14) Das Neves Gomes, C.; Jacquet, O.; Villiers, C.; Thuery, P.; Ephritikhine, M.; Cantat, T. *Angew. Chem., Int. Ed.* **2012**, *51*, 187−190.

(15) Jeoung, J.-H.; Dobbek, H. *Science* **2007**, *318*, 1461−1464.

(16) Hori, H.; Ishihara, J.; Koike, K.; Takeuchi, K.; Ibusuki, T.; Ishitani, O. *J. Photochem. Photobiol., A* **1999**, *120*, 119−124.

(17) Bolinger, C. M.; Story, N.; Sullivan, B. P.; Meyer, T. J. *Inorg. Chem.* **1988**, *27*, 4582−4587.

(18) Bruce, M. R. M.; Megehee, E.; Sullivan, B. P.; Thorp, H. H.; O'Toole, T. R.; Downard, A.; Pugh, J. R.; Meyer, T. J. *Inorg. Chem.* **1992**, 486−4873.

(19) Chen, Z.; Chen, C.; Weinber, R.; Kang, P.; Concepcion, J. J.; Harrison, D. P.; Brookhart, M. S.; Meyer, T. J. *Chem. Commun.* **2011**, *47*, 12607−12609.

(20) O'Toole, T. R.; Meyer, T. J.; Sullivan, B. P. *Chem. Mater.* **1989**, *1*, 574−576.

(21) O'Toole, T. R.; Sullivan, B. P.; Bruce, M. R. M.; Margerum, L. D.; Murray, R. W.; Meyer, T. J. *J. Electroanal. Chem. Interfacial Electrochem.* **1989**, *259*, 217−239.

(22) Pugh, J. R.; Bruce, M. R. M.; Sullivan, B. P.; Meyer, T. J. *Inorg. Chem.* **1991**, *30*, 86−91.

(23) Chen, Z.; Concepcion, J. J.; Brennaman, M. K.; Kang, P.; Norris, M. R.; Hoertz, P. G.; Meyer, T. J. *Proc. Natl. Acad. Sci. U.S.A.* **2012**, *109*, 15606−11.

(24) Chen, J.; Szalda, D. J.; Fuita, E.; Creutz, C. *Inorg. Chem.* **2010**, *49*, 9380−9391.

(25) Doherty, M. D.; Grills, D. C.; Muckerman, J. T.; Polyansky, D. E.; Fujita, E. *Coord. Chem. Rev.* **2010**, *254*, 2472−2482.

(26) Fukushima, T.; Fujita, E.; Muckerman, J. T.; Polyansky, D. E.; Tanaka, K. *238th ACS National Meeting*, 2009; p PHYS-012.

(27) Grodkowsik, J.; Dhanasekaran, T.; Neta, P.; Hambright, P.; Brunschwig, B. S.; Shinozaki, K.; Fuita, E. *J. Phys. Chem. A* **2000**, *104*, 11332−11339.

(28) Morris, A. J.; Meyer, G. J.; Fujita, E. *Acc. Chem. Res.* **2009**, *42*, 1983−1994.

(29) Benson, E. E.; Kubiak, C. P.; Sathrum, A. J.; Smieja, J. M. *Chem. Soc. Rev.* **2009**, *38*, 89−99.

(30) Haines, R. J.; Wittrig, R. E.; Kubiak, C. P. *Inorg. Chem.* **1994**, *33*, 4723−4728.

(31) Arana, C.; Yan, S.; Keshavarz-K, M.; Potts, K. T.; Abruna, H. D. *Inorg. Chem.* **1992**, *31*, 3680−3682.

(32) Chiericato, G.; Arana, C. R.; Casado, C.; Cuadrado, I.; Abruna, H. D. *Inorg. Chim. Acta* **2000**, *300*−*302*, 32−42.

(33) Hurrell, H. C.; Mogstad, A. L.; Usifer, D. A.; Potts, K. T.; Abruna, H. D. *Inorg. Chem.* **1989**, *28*, 1080−1084.

(34) Ramos, S. J. A.; Arana, C. R.; Hernandez, L.; Potts, K. T.; Keshavarz-K, M.; Abruna, H. D. *Inorg. Chem.* **1995**, *34*, 3339−3348.

(35) Barton, E. E.; Rampulla, D. M.; Bocarsly, A. B. *J. Am. Chem. Soc.* **2008**, *130*, 6342−6344.

(36) Cole, E. B.; Bocarsly, A. B. In *Carbon Dioxide as a Chemical Feedstock*; Aresta, M., Ed.; Wiley-VCH Verlag GmbH & Co. KGaA: Weinheim, 2010; pp 291−316.

(37) Cole-Barton, E.; Lakkaraju, P. S.; Rampulla, D. M.; Morris, A. J.; Abelev, E.; Bocarsly, A. B. *J. Am. Chem. Soc.* **2010**, *132*, 11539−11551.

(38) Morris, A. J.; McGibbon, R. T.; Bocarsly, A. B. *ChemSusChem* **2011**, *4*, 191−196.

(39) Seshadri, G.; Lin, C.; Bocarsly, A. B. *J. Electroanal. Chem.* **1994**, *372*, 145−150.

(40) Crabtree, R. H. In *Carbon Dioxide as Chemical Feedstock*; Aresta, M., Ed.; Wiley-VCH Verlag GmbH & Co. KGaA: Weinheim, 2010; pp 301−306.

(41) Yan, Y.; Zeitler, E. L.; Gu, J.; Hu, J.; Bocarsly, A. B. *J. Am. Chem. Soc.* **2013**, *135*, 14020−14023.

(42) Boston, D. J.; Xu, C.; Armstrong, D. W.; MacDonnell, F. M. *J. Am. Chem. Soc.* **2013**, *135*, 16252−16255.

(43) Lim, C.-H.; Holder, A. M.; Musgrave, C. B. *J. Am. Chem. Soc.* **2013**, *135*, 142−154.

(44) Keith, J. A.; Carter, E. A. *J. Am. Chem. Soc.* **2012**, *134*, 7580−7583.

(45) Ertem, M. Z.; Konezny, S. J.; Araujo, C. M.; Batista, V. S. *J. Phys. Chem. Lett.* **2013**, *4*, 745−748.

(46) Nair, R. B.; Cullum, B. M.; Murphy, C. J. *Inorg. Chem.* **1997**, *36*, 962−965.

(47) Hartshorn, R. M.; Barton, J. K. *J. Am. Chem. Soc.* **1992**, *114*, 5919−5925.

(48) Tan, L.; Xiao, Y.; Liu, X.; Zhang, S. *Spectrochim. Acta, Part A* **2009**, *73*, 858−864.

(49) Singh, S.; de Tacconi, N. R.; Diaz, N. R. G.; Lezna, R. O.; Muñoz Zuñiga, J.; Abayan, K.; MacDonnell, F. M. *Inorg. Chem.* **2011**, *50*, 9318−9328.

(50) de Tacconi, N. R.; Lezna, R. O.; Chitakunye, R.; MacDonnell, F. M. *Inorg. Chem.* **2008**, *47*, 8847−8858.

(51) Wolcan, E.; Feliz, M. R.; Ruiz, G. T.; Juliarena, M. P.; Lezna, R. O. *J. Electroanal. Chem. Interfacial Electrochem.* **2002**, *533*, 101−106.

(52) Montalti, M.; Credi, A.; Prodi, L.; Gandolfi, M. T. *Handbook of Photochemistry*, 3rd ed.; CRC Press: Boca Raton, FL, 2012.
(53) Grant, W. M. *Anal. Chem.* **1948**, *20*, 267−269.
(54) Jenkins, Y.; Friedman, A. E.; Turro, N. J.; Barton, J. K. *Biochemistry* **1992**, *31*, 10809−10816.
(55) Sun, Y.; Liu, Y.; Turro, C. *J. Am. Chem. Soc.* **2010**, *132*, 5594−5595.
(56) Sun, Y.; Turro, C. *Inorg. Chem.* **2010**, *49*, 5025−5032.
(57) Bates, W. D.; Meyer, T. J. *Inorg. Chem.* **1995**, *34*, 6421−6422.
(58) Yasukouchi, K.; Taniguchi, I.; Yasukouchi, K.; Taniguchi, I.; Yamaguchi, H.; Shiraishi, M. *J. Electroanal. Chem.* **1979**, *105*, 403−408.
(59) Skarda, V.; Cook, M. J.; Lewis, A. P.; McAuliffe, G. S. G.; Thomson, A. J. *J. Chem. Soc., Perkin Trans. 2* **1984**, *8*, 1309−1311.
(60) Fees, J.; Kaim, W.; Moscherosch, M.; Matheis, W.; Klima, J.; Krejcik, M.; Zalis, S. *Inorg. Chem.* **1993**, *32*, 166−174.
(61) Flynn, C. P. *Point Defects and Diffusion*; Clarendon Press: Oxford, 1972.
(62) Costentin, C.; Canales, J. C.; Haddou, B.; Saveant, J. M. *J. Am. Chem. Soc.* **2013**, *135*, 17671−17674.
(63) Amatore, C.; Saveant, J.-M. *J. Am. Chem. Soc.* **1981**, *103*, 5021−5023.
(64) (a) Nicholson, R. S.; Shain, I. *Anal. Chem.* **1964**, *36*, 706−723. (b) Bard, A. J.; Faulkner, L. R. *Electrochemical Methods, Fundamentals and Applications*, 2nd ed.; Wiley: New York, 2001; p 501.
(65) de Tacconi, N. R.; Chitakunye, R.; MacDonnell, F. M.; Lezna, R. O. *J. Phys. Chem. A* **2008**, *112*, 497−507.
(66) Ruiz, G. T.; Juliarena, M. P.; Lezna, R. O.; Feliz, M. R.; Ferraudi, G. *J. Photochem. Photobiol., A* **2006**, *179*, 289−297.
(67) Juliarena, M. P.; Lezna, R. O.; Feliz, M. R.; Ruiz, G. T.; Thomas, S.; Ferraudi, G.; Carmichael, I. *J. Org. Chem.* **2006**, *71*, 2870−2873.
(68) Durham, B.; Caspar, J. V.; Nagle, J. K.; Meyer, T. J. *J. Am. Chem. Soc.* **1982**, *104*, 4803−4810.
(69) Majewski, M. B.; de Tacconi, N. R.; MacDonnell, F. M.; Wolf, M. O. *Chem.—Eur. J.* **2013**, *19*, 8331−8341.
(70) Staffilani, M.; Belser, P.; Hartl, F.; Kleverlaan, C. J.; De Cola, L. *J. Phys. Chem. A* **2002**, *106*, 9242−9250.